

# Elastic Fibers Enhance the Mechanical Integrity of the Human Lumbar Anulus Fibrosus in the Radial Direction

LACHLAN J. SMITH,<sup>1,2,3</sup> SHARON BYERS,<sup>4,5</sup> JOHN J. COSTI,<sup>6</sup> and NICOLA L. FAZZALARI<sup>1,2,3</sup>

<sup>1</sup>Bone and Joint Research Laboratory, Division of Tissue Pathology, Institute of Medical and Veterinary Science, Adelaide, Australia; <sup>2</sup>Hanson Institute, Adelaide, Australia; <sup>3</sup>Discipline of Pathology, The University of Adelaide, Adelaide, Australia; <sup>4</sup>Matrix Biology Unit, Department of Genetic Medicine, Children, Youth and Women's Health Service, Adelaide, Australia; <sup>5</sup>Discipline of Paediatrics, The University of Adelaide, Adelaide, Australia; and <sup>6</sup>Department of Orthopaedics, Repatriation General Hospital and Flinders University, Adelaide, Australia

(Received 30 June 2007; accepted 29 November 2007; published online 8 December 2007)

**Abstract**—The anulus fibrosus of the human lumbar intervertebral disc has a complex, hierarchical structure comprised of collagens, proteoglycans, and elastic fibers. Recent histological studies have suggested that the elastic fiber network may play an important functional role. In this study, it was hypothesized that elastic fibers enhance the mechanical integrity of the extracellular matrix in the radial orientation, perpendicular to the plane containing the collagen fibers. Using a combination of biochemically verified enzymatic treatments and biomechanical tests, it was demonstrated that degradation of elastic fibers resulted in a significant reduction in both the initial modulus and the ultimate modulus, and a significant increase in the extensibility, of radially oriented anulus fibrosus specimens. Separate treatments and mechanical tests were used to account for any changes attributable to non-specific degradation of glycosaminoglycans. Additionally, histological assessments provided a unique perspective on structural changes in the elastic fiber network in radially oriented specimens subjected to tensile deformations. The results of this study demonstrate that elastic fibers play an important and unique role in the mechanical properties of the anulus fibrosus, and provide the basis for the development of improved material models to describe intervertebral disc mechanical behavior.

**Keywords**—Intervertebral disc, Anulus fibrosus, Elastic fibers, Elastin, Structure–function.

## INTRODUCTION

The anulus fibrosus of the human lumbar intervertebral disc has a unique hierarchical microstructure. The primary functional elements are bundles of type I collagen fibrils, arranged in discontinuous, roughly concentric lamellae around the nucleus pulposus.

Bundles are oriented obliquely to the transverse plane of the disc, with their directions alternating in each consecutive lamellae.<sup>5,27</sup> Co-distributed within this collagenous architecture is a complex network of elastic fibers.<sup>4,21,36,43</sup> Elastic fibers are critical constituents of the extracellular matrix in dynamic biological structures that functionally require elasticity and resilience, and their loss is considered to be a major cause of aging and degeneration in many tissues.<sup>22</sup> They have a complex ultrastructure, comprised of the protein elastin embedded on a microfibrillar scaffold rich in fibrillins.<sup>23</sup> Immunohistochemical analysis has demonstrated that both elastin and fibrillin-1 are widely distributed throughout the anulus fibrosus.<sup>44</sup> The arrangement of elastic fibers in the anulus is distinct at each level of the collagen structural hierarchy: within lamellae, they are arranged parallel to the collagen fibers; at lamellar interfaces they form discrete connections between collagen bundles in consecutive lamellae.<sup>36</sup> There is also evidence that elastic fibers form ‘cross-bridges’ to connect collagen bundles in non-consecutive lamellae.<sup>44,45</sup> The density of elastic fibers within the lamellae is heterogeneous both radially and circumferentially. Density is higher in the lamellae of the outer anulus than in those of the inner, and higher in the lamellae of the posterolateral region than in those of the anterolateral.<sup>36</sup> Elastic and collagenous elements are embedded in a hydrated ground matrix rich in glycosaminoglycans.<sup>38</sup>

The mechanical function of the anulus fibrosus is twofold: to provide mobility to the spine by facilitating flexion, extension, lateral bending and twisting, and to resist the radial forces generated by the bulging of the nucleus pulposus under compressive loads.<sup>24</sup> As a consequence, the anulus fibrosus is subjected to complex strains; its anisotropic mechanical properties reflect this, and have been quantified extensively at the

Address correspondence to Lachlan J. Smith, Bone and Joint Research Laboratory, Division of Tissue Pathology, Institute of Medical and Veterinary Science, Adelaide, Australia. Electronic mail: lachlan.smith@imvs.sa.gov.au

tissue level.<sup>7,9,11,13,17</sup> Parallel to the direction of the collagen fiber bundles, high elastic modulus reflects the dominant mechanical role of the collagen fibers. Perpendicular to the direction of the bundles modulus values are approximately two orders of magnitude smaller, suggesting a more central mechanical role for non-collagenous elements such as elastic fibers, which possess low elastic modulus, high extensibility, and high resilience.<sup>9,11,12,17</sup>

Detailed histological analyses of the elastic fiber network structure have provided an initial framework enabling researchers to hypothesize as to their possible functional roles, and it has been suggested that elastic fibers may play a critical role in reinforcing the mechanical integrity of the collagen matrix and in facilitating its elastic recoil, both within and between collagen fiber bundles; however, there is currently no experimental evidence to support these theories.<sup>18,36,44,45</sup>

Targeted enzymatic treatments have been used extensively in combination with biomechanical testing to stratify both tensile and compressive mechanical properties of connective tissues in terms of the individual contributions of elastic fibers and other constituents such as glycosaminoglycans.<sup>25,30–32,35</sup> The objective of this investigation was to apply such techniques to study the role of elastic fibers in the tensile mechanical properties of the anulus fibrosus. It was hypothesized that elastic fibers enhance the mechanical integrity of the anulus in the radial orientation, perpendicular to the plane containing the collagen fibers. Specimens from both anterolateral and posterolateral quadrants were studied, facilitating an analysis of circumferential heterogeneity, and specimens from discs of varying morphological grades were assessed for evidence of degeneration-related dependence. Additionally, histological techniques were used to assess changes to the elastic fiber network structure in specimens clamped and fixed under tensile strains, providing mechanical testing results with a complementary structural perspective.

## MATERIALS AND METHODS

### *Specimen Preparation*

Eight human lumbar spines from cases ranging in age from 16 to 87 years were harvested at autopsy within 24 h of death, with research ethics committee and next-of-kin approvals. Whole intervertebral discs from the L1–L2 level were removed at the endplates using a scalpel. Discs were hemi-sected mid-sagittally and macroscopically graded by two independent assessors for degenerative condition using a modified Thompson scheme.<sup>39</sup> Of these discs two each were assigned grades

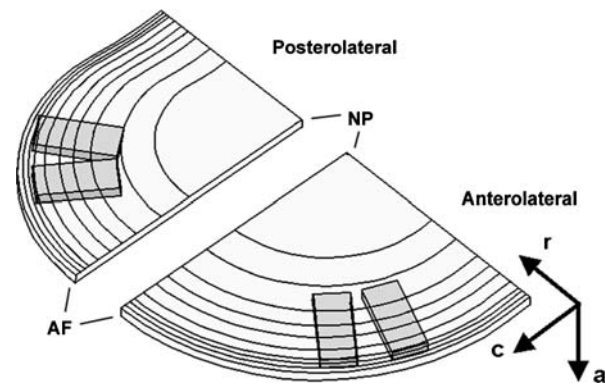


**FIGURE 1.** Schematic representation of specimen harvest sites in the anterolateral and posterolateral quadrants of the anulus fibrosus. AF = anulus fibrosus, NP = nucleus pulposus; r, a, and c indicate radial, axial, and circumferential directions, respectively.

of one (aged 16 and 40), two (aged 28 and 57), three (aged 66 and 76), and four (aged 80 and 87).

Each hemi-disc was then divided into an anterolateral and posterolateral quadrant, and the nucleus was separated from the anulus at the transition zone using a scalpel and discarded. Quadrants, aligned with the mid-axial plane of the disc, were trimmed incrementally using a cryostat until a uniform thickness of approximately 2 mm was achieved. Two parallel strips, approximately 5 mm wide, were cut from each quadrant (Fig. 1) using a parallel-edged razor-tool, and trimmed to an approximate length of 10 mm. The length of each specimen extended approximately from the disc periphery to the transition zone, with the central gauge region located approximately in the middle anulus. Specimens were equilibrated in 0.15 M phosphate buffer saline for 1 h at 4 °C, after which width and thickness were measured optically using a digital vision system with a resolution of  $\pm 10 \mu\text{m}$ . Dimension measurements were made both prior and subsequent to enzymatic treatments.

### *Enzymatic Treatments and Biochemical Validation*

Elastin, the core constituent of elastic fibers, was selectively degraded from the tissue matrix using an optimized version of established techniques.<sup>25,28,30</sup> One specimen from each quadrant was incubated in a solution consisting of 3 U of high purity pancreatic elastase in 1 mL of 0.2 M Tris-HCl, pH 8.6, with 10 mM N-ethylmaleimide and 5 mM benzamidine hydrochloride as protease inhibitors. Additionally, 3 mg of soybean trypsin inhibitor was included to limit non-specific degradation of collagen by the elastase.<sup>28</sup> To account for the predicted effects of non-specific degradation of glycosaminoglycans by elastase, the second, adjacent specimen from each quadrant was

incubated in a solution consisting of 1 U of chondroitinase ABC in 1 mL of 0.05 M Tris-HCl plus 0.06 M sodium acetate buffer, pH 8.0, with 10 mM N-ethylmaleimide and 5 mM benzamidine hydrochloride and 1 mM phenylmethanesulfonyl fluoride as protease inhibitors, to specifically degrade glycosaminoglycans while leaving elastic fibers and collagen unaffected. Both treatments were carried out for 36 h at 37 °C with gentle agitation. Following treatment, specimens were washed for 30 min in 0.15 M phosphate buffered saline; washes were then combined with extracts for biochemical analyses as required. All reagents were obtained from Sigma-Aldrich, St Louis, MO, USA.

The efficacy of the enzyme treatments was validated biochemically in a preliminary study. The degradation of elastin by the elastase treatment was assessed using a competitive enzyme immunoassay (ELISA) for desmosine, a tetrafunctional crosslinking amino acid unique to elastin.<sup>23</sup> The assay methodology was adapted from established techniques.<sup>29,42</sup> Degradation of triple-helical collagen by elastase was assessed by measuring hydroxyproline.<sup>37</sup> Degradation of hydroxylysylpyridinium crosslinks (pyridinoline) from collagen by elastase was measured using an adaptation of an established reversed-phase high performance liquid chromatographic (HPLC) technique.<sup>10</sup> Glycosaminoglycan degradation in specimens treated with elastase or chondroitinase ABC was assessed by measurement of uronic acid.<sup>3</sup> Prior to assays being conducted, treated tissue fragments were completely digested for 24 h at 56 °C in 2 mL of a solution containing 100 µg of proteinase K buffered with 100 mM di-potassium hydrogen orthophosphate at pH 8.0. 1 mL each of proteinase K digested tissues, and combined extracts plus wash solutions were then subjected to 24 h of hydrolysis in 6 M hydrochloric acid at 110 °C. Aliquots of hydrolyzed solutions were used for desmosine, hydroxyproline, and pyridinoline assays. Aliquots of unhydrolyzed solutions were used for uronic acid assays.

### Mechanical Testing

To facilitate precise mounting of specimens in the grips of the testing machine, a 2-piece disposable frame was constructed for each specimen from 150 grit silicon carbide polishing paper (Fig. 2). Polystyrene spacers were glued to the corners of each frame to ensure the gripping force was evenly distributed over the surface of the specimen ends and to prevent crushing. Before mounting in the grips of the mechanical testing system, the two parts of the frame were combined to form a sandwich over the specimen and fixed in position using fast drying adhesive. The initial gauge region, defined as the frame window height measured using digital callipers, was  $2.19 \pm 0.11$  mm.

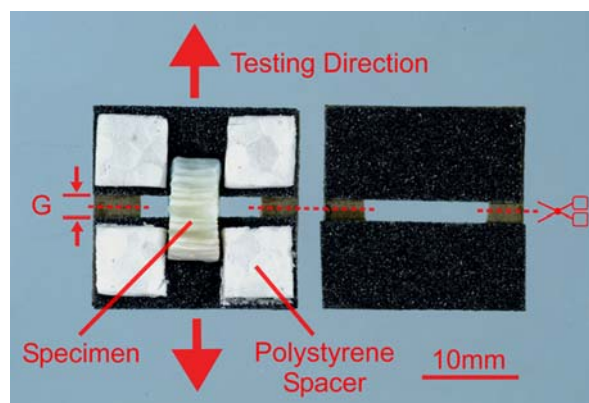


**FIGURE 2.** Sandpaper mounting frame (prior to assembly) with specimen in position. G = gauge region; dotted lines = cutting zones following placement in the mechanical testing system grips.

Each specimen was initially re-equilibrated in 0.15 M phosphate buffer saline at 4 °C for 1 h, then mounted in a frame which was in turn placed in the grips of the mechanical testing system (Mach-1 A400; Biosyntech, Laval, Canada), and the frame sides were cut. The system had a displacement resolution of 0.5 µm and a load cell resolution of 0.005 N. Specimens were tested while submerged in a 0.15 M phosphate buffered saline bath to prevent dehydration. Five cycles of preconditioning using a triangular waveform were initially applied at a strain rate of 0.05 s<sup>-1</sup> under displacement control, after which the response was observed to be repeatable. A single ramp at a constant strain rate of 0.0025 s<sup>-1</sup> was then applied, for calculation of quasi-static mechanical properties. This testing protocol was repeated following enzymatic treatment for each specimen. Gauge regions were relocated precisely using the high resolution images previously obtained for specimen dimension analysis as a guide. It was critical that the maximum strain amplitude used for quasi-static tests exceed the extensibility of specimens to permit determination of ultimate modulus, but significantly precede the yield strain to enable repeat testing. Preliminary work and the results of a previous study suggested a high level of inter-specimen variability with respect to these properties.<sup>11</sup> The optimum maximum strain amplitudes were therefore determined experimentally for each specimen immediately prior to preconditioning, by applying a constant strain rate ramp at 0.05 s<sup>-1</sup> until the response was observed to exceed the transition strain and enter the second linear region. Maximum strain amplitudes were  $0.31 \pm 0.11$ ,  $0.46 \pm 0.19$ , and  $1.22 \pm 0.50$  mm/mm for pre-treatment, and following chondroitinase ABC and elastase treatments, respectively (mean ± SD).

Engineering stress (force divided by undeformed cross-sectional area at equilibrium hydration) vs. strain



(the instantaneous length divided by the starting length) was plotted for each specimen before and after treatment. Post-treatment cross-sectional areas were calculated using post-treatment dimensions. Initial modulus (tangent to the toe region of the response), ultimate modulus (tangent to the second linear region of the response) and extensibility (corresponding to the strain at the point of transition between the toe and second linear regions), illustrated in Fig. 3, were calculated from the raw data. Previous studies of anulus quasi-static mechanical properties have defined elastic modulus either as the tangent to the linear region of the curve at a prescribed percentage of the yield strain, or using moving cell linear regression, in which the regression line with the optimum coefficient of determination defines the modulus.<sup>7,11</sup> As the testing in this study was non-destructive, the second of these methods was adopted. For ultimate modulus, regression commenced at the maximum strain; for initial modulus, the regression started at zero strain. Extensibility, defined as the transition strain between the first and second linear regions, was calculated as the intersection point of tangents to these two regions (Fig. 3).

The repeatability of the mechanical testing protocol was assessed in a preliminary study. Four specimens, separate from those allocated to the primary treatment groups, were tested non-destructively using the methods outlined. They were then removed from the clamps and re-equilibrated in phosphate buffered saline for approximately 1 h, considered sufficiently long for fluid and tissue elements to return to their pre-test homeostatic configuration, but sufficiently short to prevent significant loss of glycosaminoglycans through ionic diffusion, then retested using the same protocol. Initial modulus, ultimate modulus, and extensibility were compared for the initial and repeat tests using paired Student's *t*-tests, and any significant differences reported for two-tailed *p* values less than 0.05.

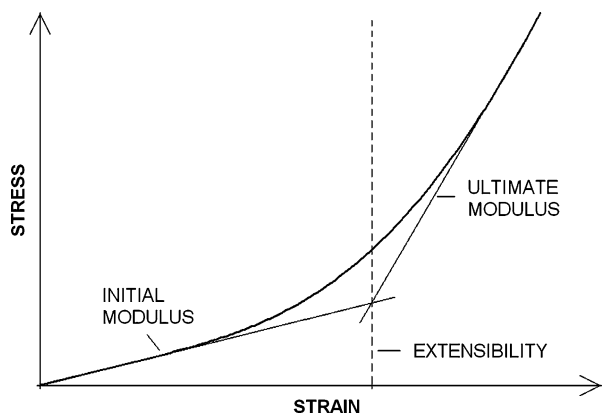


**FIGURE 3.** Mechanical properties—initial modulus, ultimate modulus, and extensibility—as they relate to each region of the quasi-static stress–strain response.

### Data Analysis

Paired mechanical testing data sets, before and after treatments, were assessed separately for normality using the Shapiro–Wilk test. Statistical differences for each property (initial modulus, ultimate modulus, and extensibility) between pre-treatment and post-treatment measurements were assessed using paired Student's *t*-tests where data were normally distributed (expressed as mean  $\pm$  standard deviation), or using the Wilcoxon signed ranks test where data were non-parametric (expressed as median, interquartile range). Likewise, paired tests were used to compare the effect of region (anterolateral vs. posterolateral), and Student's *t*-tests or Mann–Whitney *U* tests were used to assess the effect of degeneration (specimens grouped as grade 1 or 2 vs. grade 3 or 4) on mechanical properties. Significance was reported for 2-tailed *p* values less than 0.05. Statistical analyses were performed using GraphPad Prism V5 (GraphPad Software Inc., San Diego, CA, USA).

### Histological Assessment

Four specimens, prepared as described from two additional non-degenerate hemi-discs, were subjected to non-destructive peak strains determined as for mechanical tests, then clamped whilst fully extended and fixed overnight in 10% buffered formalin. Specimens were then routinely processed and paraffin embedded. Sections 30  $\mu\text{m}$  thick were cut from the surface parallel to the axial plane of the disc, and mounted on gelatin coated microscope slides. Sections were rehydrated through xylenes and progressive alcohols to distilled water, oxidized with potassium permanganate, decolorized with oxalic acid, and stained with resorcin-fuchsin. Tissue structure was assessed on a light microscope attached to an imaging workstation (Leica Microsystems, Wetzlar, Germany), at an objective magnification of 100 times. Elastic fiber network structure within collagen bundles and at lamellar boundaries was visualized using phase contrast, composite z-stack imaging.<sup>36</sup> Finally, patterns of fiber arrangement in the loaded specimens were compared with those observed in unloaded specimens.

## RESULTS

### Biochemical Validation

Treatment with elastase resulted in  $68.2 \pm 15.4$  (mean  $\pm$  SD) percent degradation of elastin, measured as crosslinking desmosine. Degradation of triple-helical collagen by the elastase treatment, measured as hydroxyproline, was small ( $4.6 \pm 1.7\%$ ), as was

degradation of collagen crosslinks, measured as pyridinoline ( $4.0 \pm 1.9\%$ ). The degrees of hydroxyproline degradation and pyridinoline degradation were highly correlated ( $r = 0.80$ ). Elastase and chondroitinase ABC treatments both removed the majority of glycosaminoglycans ( $91.9 \pm 1.7\%$  and  $71.9 \pm 4.5\%$ , respectively), measured as uronic acid.

### Mechanical Testing

Untreated specimens subjected to repeat testing following 1 h of re-equilibration displayed no significant change in initial modulus ( $p = 0.4$ ), ultimate modulus ( $p = 0.6$ ), or extensibility ( $p = 0.2$ ), thereby validating the repeatability of the test protocol.

Results from four specimens were discarded due to artefacts in their respective load vs. displacement characteristics. The effects of elastase treatment on tissue mechanical properties are illustrated in Fig. 4a. Following treatment, initial modulus decreased by 93%, ultimate modulus decreased by 91% and extensibility increased by 431%. In all cases the change was significant ( $p < 0.001$ ). The effects of chondroitinase ABC treatment on tissue mechanical properties are illustrated in Fig. 4b. Following treatment, initial modulus decreased by 49% and extensibility increased by 69% (both changes significant,  $p < 0.001$ ). There was no significant change in ultimate modulus. All percentages stated are median values. The magnitudes of the changes in both initial modulus and extensibility were significantly different between elastase and chondroitinase ABC treated groups ( $p < 0.001$  for both).

A comparison of mechanical testing results prior to treatment between anterolateral (AL) and posterolateral (PL) quadrants revealed no significant differences for initial modulus (AL:  $0.096 \pm 0.062$  MPa, PL:  $0.055 \pm 0.040$  MPa, mean  $\pm$  SD,  $p = 0.11$ ) or ultimate modulus (AL:  $0.272 \pm 0.178$  MPa, PL:  $0.167 \pm 0.103$  MPa,  $p = 0.17$ ), although observed trends suggested that both tended to be higher for anterolateral specimens. Extensibility was found to be significantly higher for posterolateral specimens (AL:  $0.149 \pm 0.016$  mm/mm, PL:  $0.223 \pm 0.081$  mm/mm,  $p = 0.02$ ). Following treatment with elastase, differences in initial and ultimate modulus between regions remained insignificant ( $p = 0.55$  and  $p = 0.16$ , respectively), and extensibility remained significantly higher for posterolateral specimens ( $p = 0.02$ ). Following treatment with chondroitinase ABC, there were no significant differences in any of the properties between regions, however observed trends suggested posterolateral specimens maintained higher extensibility ( $p = 0.11$ ), while anterolateral specimens maintained a higher initial modulus ( $p = 0.08$ ). With respect to the magnitudes of the changes observed in each of the mechanical properties, no significant differences or trends were observed between the two regions for either treatment.

Correlation between age and disc condition was high and significant ( $r = 0.90$ ,  $p = 0.002$ ), making these factors indistinguishable for the purposes of analysis. To compare the effects of degeneration on mechanical properties, specimens were grouped as either non-degenerate (grade 1 and 2) or as degenerate

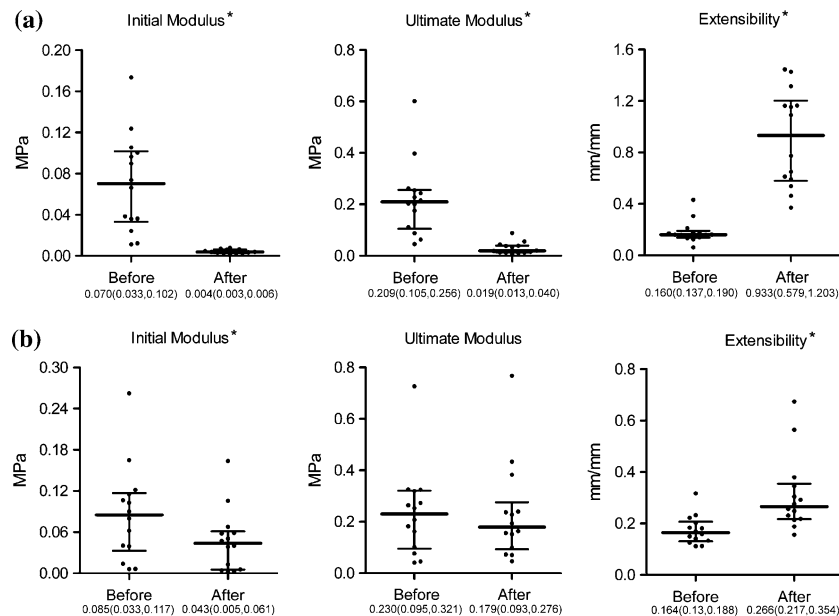


**FIGURE 4.** (a) Initial modulus, ultimate modulus, and extensibility before and after elastase treatment. (b) Initial modulus, ultimate modulus, and extensibility before and after chondroitinase ABC treatment (median and interquartile range). \* Indicates significant difference before and after treatment,  $p < 0.001$ .

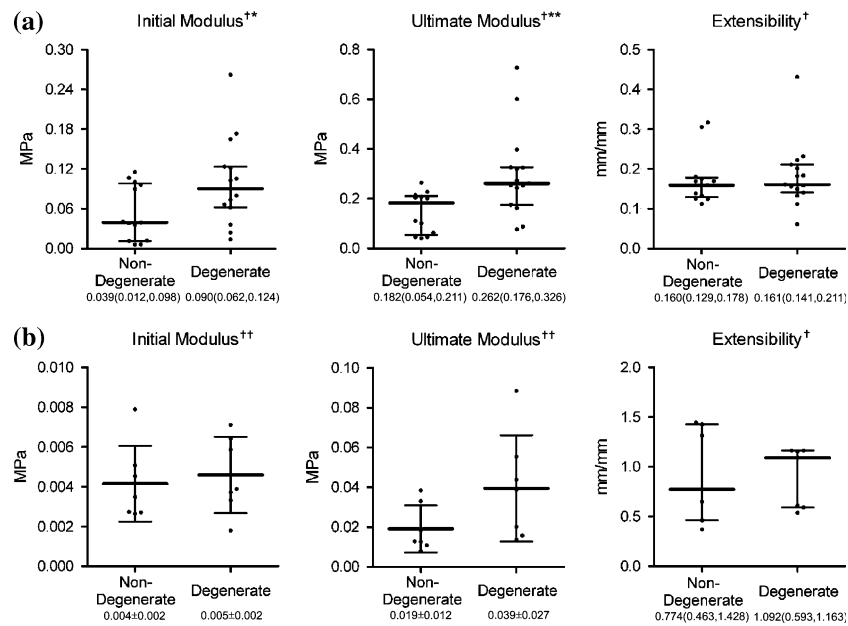


**FIGURE 5.** Comparisons of initial modulus, ultimate modulus, and extensibility between non-degenerate and degenerate specimens for (a) untreated specimens and (b) elastase treated specimens. † Median and interquartile range; †† mean  $\pm$  standard deviation; \* significant difference,  $p < 0.05$ , \*\*  $p < 0.005$ .

(grade 3 and 4). Prior to treatment, initial modulus was significantly greater for degenerate specimens ( $p = 0.046$ ), as was ultimate modulus ( $p = 0.004$ ) (Fig. 5a). No significant difference in extensibility was found between non-degenerate and degenerate groups. Following elastase treatment, no significant difference were observed for any of the properties between groups, however, a trend remained for ultimate modulus to be higher for degenerate specimens ( $p = 0.09$ ) (Fig. 5b). Following chondroitinase ABC treatment, no significant differences were observed between groups, although trends suggested initial modulus remained greater for degenerate specimens ( $p = 0.11$ ). An analysis of the magnitudes of the changes in each of the properties revealed no significant differences between non-degenerate and degenerate groups for either treatment.

#### Histological Assessment

Within the collagen bundles of radial specimens subjected to tensile strains, two distinct patterns of fiber behavior were apparent: fibers aligning towards the loading direction appeared long and straight, as if in tension; fibers aligning more perpendicular to the loading direction appeared short and relaxed, or ‘crumpled’, as if in compression (Fig. 6). This pattern of fiber distribution (Fig. 7a) is distinct when compared to that observed in unloaded specimens (Fig. 7b), where elastic fibers are aligned predominantly parallel to the direction of the collagen fibers. At lamellar

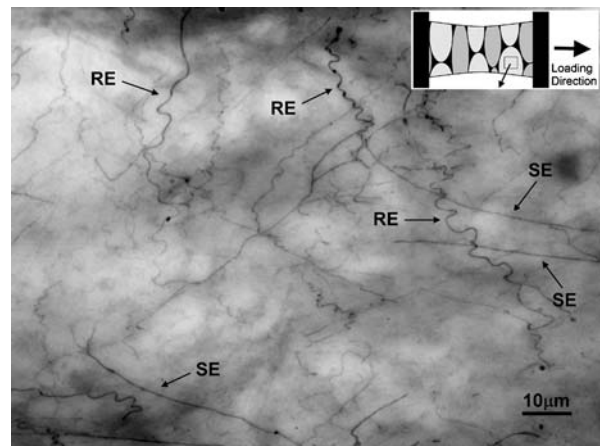


**FIGURE 6.** Elastic fiber network structure within a collagen bundle, in a specimen under tensile strain (inset schematic shows loading direction). SE = straight elastic fibers indicate tension; RE = relaxed elastic fibers indicate compression (Resorcin-fuchsin stain, phase contrast composite z-stack image, 100 $\times$  objective magnification).

interfaces, discrete bundles of elastic fibers were observed to form points of adhesion between otherwise separating lamellae (Fig. 8).

#### DISCUSSION

Descriptions of structure–function relationships within the extracellular matrix of soft biological tissues such as the anulus fibrosus are important for several reasons: they enable researchers to understand, model

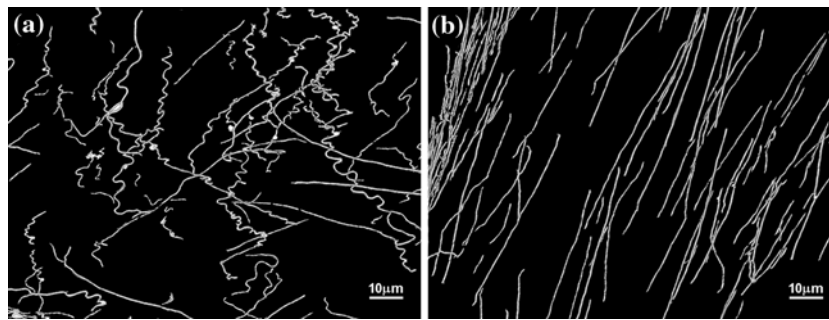


**FIGURE 7.** Comparison of elastic fiber arrangements within the collagen bundles of loaded and unloaded specimens. (a) Elastic fiber arrangement in a collagen bundle of a radial specimen under tensile strain (the same location shown in Fig. 6, but the image has been binarised and inverted to highlight fiber alignments). (b) Elastic fiber arrangement in a collagen bundle of a specimen subjected to zero strain. Original images were z-series projections taken from 30  $\mu\text{m}$ -thick sections stained with resorcin-fuchsin and imaged under phase contrast at 100 times objective magnification.

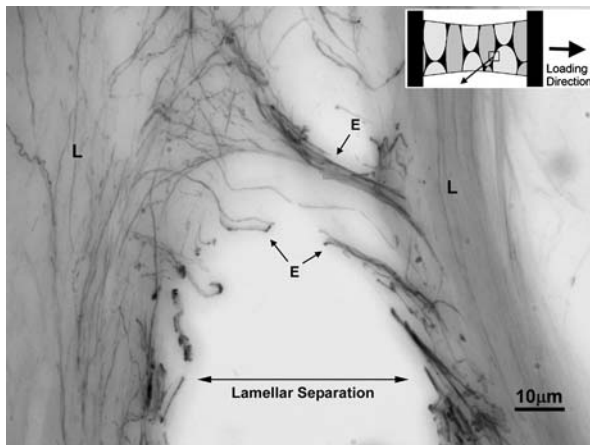


**FIGURE 8.** Bundles of elastic fibers, E, forming connections between two collagen bundles in consecutive lamellae, L, undergoing transverse separation, in a radial specimen under strain (inset schematic shows loading direction) (Resorcin-fuchsin stain, phase contrast composite z-stack image, 100 $\times$  objective magnification).

and predict mechanical damage; they highlight potential therapeutic targets for slowing or reversing the degenerative process; and they aid efforts to successfully engineer functionally accurate synthetic and biological tissue replacements. In this study, experimental data are presented describing the nature and magnitude of the contributions made by elastic fibers to the quasi-static tensile mechanical properties of the annulus in the radial direction. This was achieved using a combination of biochemically verified targeted enzymatic treatments combined with biomechanical tests. Additionally, histological evidence of the structural behavior of elastic fibers in radial deformation both within collagen bundles and at lamellar interfaces is presented.

Elastase treatment resulted in some unavoidable non-specific degradation of collagen despite the inclusion of soybean trypsin inhibitor. This small loss was

considered unlikely to have confounded results both due to the significance of the observed changes in mechanical properties and the fact that specimens were tested perpendicular to the principle stress axis of the collagen fibers. Additionally, a previous study using similar techniques reported no effect on the mechanical properties of pure collagen, despite minor biochemical changes.<sup>28</sup> As demonstrated by biochemical analyses, degradation of matrix components by enzymatic treatments was not absolute. Variability in the amount of elastin (measured as desmosine) was particularly high, making possible differences in results with both region and condition more difficult to elucidate. Annulus mechanical properties in the radial orientation have been shown to be radially heterogeneous.<sup>11</sup> The fact that radial position was not strictly controlled may have therefore contributed to the high variances associated with pre-treatment mechanical properties. The strain rate that was used for the quasi-static ramp tests is comparatively high—as the annulus matrix comprises both solid and fluid phases, a strain rate which exceeds the maximum flow rate of the fluid phase may somewhat exaggerate the initial modulus of the solid phase. This fact was considered unlikely to reflect on the validity of the results due to the comparative nature of the analyses. Additionally, there is evidence that the tensile response of radial specimens is not strain rate dependant.<sup>11</sup> Finally, the sample size of eight intervertebral discs was quite small, however the inclusion of repeated measurements within each disc, and the significance of the observed changes suggests that it was sufficiently powerful to satisfy the core hypothesis. It is possible that with slightly greater numbers, some trends observed in regional and condition comparisons may have become significant.

Modulus values determined in this study compare favorably with those determined previously for radially oriented specimens, with any differences likely attributable to dissimilarities in specimen preparation



techniques, and whether dimensions were measured before or after saline equilibration.<sup>9,11,26</sup> It is also possible that the semi-qualitative nature of method used to define the maximum strain, in which particular care was taken not to exceed the yield strain of the tissue, may have resulted in slight underestimation of ultimate modulus, although the results of the repeatability study suggest the technique was effective. Importantly, modulus values are also comparable to those determined for single lamellar, circumferential plane specimens tested perpendicular to the collagen fiber direction.<sup>17</sup>

Following treatment with elastase, specimens exhibited large and significant reductions in initial and ultimate modulus, and increases in extensibility. Following treatment with chondroitinase ABC, specimens exhibited significant, although much more moderate respective reductions in initial modulus and increases in extensibility, and no significant change in ultimate modulus. Respective decreases in modulus and increases in extensibility following elastase treatment suggest that elastic fibers function to guide and restrain the deformation of the collagen matrix, and that on their removal, collagenous elements are able to separate and rearrange more easily and to a greater extent.

While previous studies have used enzymatic degradation to demonstrate important relationships between glycosaminoglycan content and compressive modulus and permeability, this study is the first to demonstrate that the tensile role of glycosaminoglycans is also significant, specifically with respect to initial modulus and extensibility.<sup>31,32</sup> This suggests that any age related decrease in glycosaminoglycan content may reduce the shock-absorbing capacity of the anulus matrix in tension as well as compression. The role of glycosaminoglycans appears to be distinct in nature and magnitude from that of elastic fibers, which were found to enhance initial elastic modulus and limit extensibility to a greater extent, as well as maintain the mechanical integrity of the collagen matrix at higher relative stresses.

Extensibilities of untreated specimens (Fig. 4) were generally greater than the mean radial tensile strains which occur in the anulus during physiological loading due to nuclear expansion and migration, which range from 4.7 to 9.8% depending on circumferential position, degenerative condition and loading modality.<sup>40</sup> This suggests that physiological radial strains occur predominantly within the initial toe region. Extensibility was found to be significantly greater for posterolateral specimens, both before and after elastase treatment. This suggests that neither elastic fibers nor glycosaminoglycans are directly responsible, and that it is more likely to be a result of variations in collagenous architecture, which has been demonstrated to be

of greater complexity in the posterolateral region.<sup>41</sup> This represents an important, and until now unreported structure–function association, which may reflect the greater, and more complex physiological stresses and strains experienced by this region of the anulus.<sup>8,34</sup> Elastic fiber density was recently shown to be greater in this region of the disc, possibly enabling the matrix to recover from larger and more complex deformations.<sup>36</sup> This may represent a mechanobiological or evolutionary response designed to enhance the mechanical integrity in this region, a common site for radial fissures leading to nuclear prolapse.<sup>16</sup>

The tensile mechanical properties of the anulus fibrosus at the tissue level have been shown previously to exhibit dependence on degenerative condition: in the circumferential orientation Poisson's ratio, failure stress, strain energy density, elastic modulus and fiber reorientation are all influenced by degeneration.<sup>1,14</sup> The results of this study extend these findings to the radial orientation, demonstrating that both initial modulus and ultimate modulus are higher for degenerate specimens. Physiologically, both radial and circumferential strain magnitudes are greater in degenerate discs.<sup>40</sup> A consequence of higher physiological strains combined with a stiffer matrix may be the increased likelihood of mechanical damage manifested as matrix cracking and delamination.<sup>19</sup> It is possible that these changes occur as a consequence of the spatial alterations in stress distribution that occur with degeneration.<sup>2</sup> The elastin content of the anulus has recently been shown to increase with degeneration, possibly representing a functional adaptation to reinforce collagen matrix cohesion in response to such changes in stress distribution.<sup>6</sup> Further studies are required to determine whether this increase in elastin occurs within collagen bundles, at lamellar interfaces or both.

Our histological results are consistent with recent observations that radial deformation occurs as a result of both transverse bundle deformation and lamellar separation.<sup>33</sup> Within collagen bundles, elastic fibers exhibited multiple patterns of rearrangement. Some appeared long and straight, as if in tension, while others appeared crumpled, as if in compression, suggesting that they are capable of resisting strains applied in multiple dimensions. At lamellar interfaces, bundles of elastic fibers were observed linking separating lamellae, suggesting they play a critical role maintaining lamellar cohesion. Evidence that fatigue related damage is commonly manifested as separation of anulus lamellae highlights the potential importance of these connections.<sup>20</sup>

While in this investigation radially oriented specimens were studied, as implied by our hypothesis, the results as they pertain to the functional role of elastic



fibers may be equally applicable to any specimen orientation where deformation occurs by way of transverse separation and rearrangement of collagenous elements. The fact that quasi-static properties of specimens oriented parallel to the circumferential surface of the disc and tested perpendicular to the collagen bundle direction are comparable to those determined in this study supports this theory.<sup>17</sup>

Finally, our results provide the basis for the development of new and improved material models to accurately describe the mechanical behavior of the intervertebral disc in terms of the individual contributions of its extracellular constituents. A model was recently proposed for the annulus fibrosus which included terms representing the contributions of collagen fibers, extrafibrillar ground matrix, and fiber-matrix interactions provided by non-collagenous constituents.<sup>15</sup> This model predicted that normal and shear interactions regulated by these constituents contribute significantly to multi-dimensional annulus fibrosus mechanical behavior. The results presented here provide experimental evidence of the nature and extent of that contribution, and identify elastic fibers as a major interactive structural candidate. Further studies are required to determine the nature and extent of their contribution in other orientations.

#### ACKNOWLEDGMENTS

Funding for this study was provided by the National Health and Medical Research Council, the University of Adelaide and the Institute of Medical and Veterinary Science. Donation of cadaveric material is gratefully acknowledged. The authors additionally acknowledge Professor William Walsh for providing access to his mechanical testing facilities, and Mr Enzo Ranieri, Dr Peter Clements and Mr Richard Stanley for their assistance with specific technical aspects.

#### REFERENCES

- <sup>1</sup>Acaroglu, E. R., J. C. Iatridis, L. A. Setton, R. J. Foster, V. C. Mow, and M. Weidenbaum. Degeneration and aging affect the tensile behavior of human lumbar annulus fibrosus. *Spine* 20:2690–2701, 1995.
- <sup>2</sup>Adams, M. A., D. S. McNally, and P. Dolan. ‘Stress’ distributions inside intervertebral discs. The effects of age and degeneration. *J. Bone Joint Surg. Br.* 78:965–972, 1996.
- <sup>3</sup>Blumenkrantz, N., and G. Asboe-Hansen. New method for quantitative determination of uronic acids. *Anal. Biochem.* 54:484–489, 1973.
- <sup>4</sup>Buckwalter, J. A., R. R. Cooper, and J. A. Maynard. Elastic fibers in human intervertebral discs. *J. Bone Joint Surg. Am.* 58:73–76, 1976.
- <sup>5</sup>Cassidy, J. J., A. Hiltner, and E. Baer. Hierarchical structure of the intervertebral disc. *Conn. Tissue Res.* 23:75–88, 1989.
- <sup>6</sup>Cloyd, J. M., and D. M. Elliott. Elastin content correlates with human disc degeneration in the annulus fibrosus and nucleus pulposus. *Spine* 32:1826–1831, 2007.
- <sup>7</sup>Ebara, S., J. C. Iatridis, L. A. Setton, R. J. Foster, V. C. Mow, and M. Weidenbaum. Tensile properties of nondegenerate human lumbar annulus fibrosus. *Spine* 21:452–461, 1996.
- <sup>8</sup>Edwards, W. T., N. R. Ordway, Y. Zheng, G. McCullen, Z. Han, and H. A. Yuan. Peak stresses observed in the posterior lateral annulus. *Spine* 26:1753–1759, 2001.
- <sup>9</sup>Elliott, D. M., and L. A. Setton. Anisotropic and inhomogeneous tensile behavior of the human annulus fibrosus: experimental measurement and material model predictions. *J. Biomech. Eng.* 123:256–263, 2001.
- <sup>10</sup>Eyre, D. R., T. J. Koob, and K. P. Van Ness. Quantitation of hydroxypyridinium crosslinks in collagen by high-performance liquid chromatography. *Anal. Biochem.* 137:380–388, 1984.
- <sup>11</sup>Fujita, Y., N. A. Duncan, and J. C. Lotz. Radial tensile properties of the lumbar annulus fibrosus are site and degeneration dependent. *J. Orth. Res.* 15:814–819, 1997.
- <sup>12</sup>Fung, Y. C. *Biomechanics: Mechanical Properties of Living Tissues*. New York: Springer-Verlag, 433 pp, 1981.
- <sup>13</sup>Galante, J. O. Tensile properties of the human lumbar annulus fibrosus. *Acta Orthop. Scand. Suppl* 100:1–91, 1967.
- <sup>14</sup>Guerin, H. A. L., and D. M. Elliott. Degeneration affects the fiber reorientation of human annulus fibrosus under tensile load. *J. Biomech.* 39:1410–1418, 2006.
- <sup>15</sup>Guerin, H. L., and D. M. Elliott. Quantifying the contributions of structure to annulus fibrosus mechanical function using a nonlinear, anisotropic, hyperelastic model. *J. Orth. Res.* 25:508–516, 2007.
- <sup>16</sup>Haefeli, M., F. Kalberer, D. Saegesser, A. Nerlich, N. Boos, and G. Paesold. The course of macroscopic degeneration in the human lumbar intervertebral disc. *Spine* 31:1522–1531, 2006.
- <sup>17</sup>Holzappel, G. A., C. A. J. Schulze-Bauer, G. Feigl, and P. Regitnig. Single lamellar mechanics of the human lumbar annulus fibrosus. *Biomech. Model. Mechanobiol.* 3:125–140, 2004.
- <sup>18</sup>Humzah, M. D., and R. W. Soames. Human intervertebral disc: structure and function. *Anat. Rec.* 220:337–356, 1988.
- <sup>19</sup>Iatridis, J. C., and I. ap Gwynn. Mechanisms for mechanical damage in the intervertebral disc annulus fibrosus. *J. Biomech.* 37:1165–1175, 2004.
- <sup>20</sup>Iatridis, J. C., J. J. MacLean, and D. A. Ryan. Mechanical damage to the intervertebral disc annulus fibrosus subjected to tensile loading. *J. Biomech.* 38:557–565, 2005.
- <sup>21</sup>Johnson, E. F., H. Berryman, R. Mitchell, and W. B. Wood. Elastic fibres in the annulus fibrosus of the adult human lumbar intervertebral disc. A preliminary report. *J. Anat.* 143:57–63, 1985.
- <sup>22</sup>Kielty, C. M. Elastic fibres in health and disease. *Expert Rev. Mol. Med.* 8:1–23, 2006.
- <sup>23</sup>Kielty, C. M., M. J. Sherratt, and C. A. Shuttleworth. Elastic fibres. *J. Cell Sci.* 115:2817–2828, 2002.
- <sup>24</sup>Langrana, N. A., and W. T. M. Edwards Sharma. Biomechanical analysis of loads of the lumbar spine. In: *The Lumbar Spine*, edited by S. W. Wiesel, J. N. Weinstein, H. N. Herkowitz, J. Dvorak, and G. Bell. Philadelphia: Saunders, 1996, pp. 163–181.

- <sup>25</sup>Lee, T. C., R. J. Midura, V. C. Hascall, and I. Vesely. The effect of elastin damage on the mechanics of the aortic valve. *J. Biomech.* 34:203–210, 2001.
- <sup>26</sup>Marchand, F., and A. M. Ahmed. Mechanical properties and failure mechanisms of the lumbar disc annulus. *Trans. Orth. Res. Soc.* 14:355, 1989.
- <sup>27</sup>Marchand, F., and A. M. Ahmed. Investigation of the laminate structure of lumbar disc anulus fibrosus. *Spine* 15:402–410, 1990.
- <sup>28</sup>Missirlis, Y. F. Use of enzymolysis techniques in studying the mechanical properties of connective tissue components. *J. Bioeng.* 1:215–222, 1977.
- <sup>29</sup>Osakabe, T., Y. Seyama, and S. Yamashita. Comparison of ELISA and HPLC for the determination of desmosine or isodesmosine in aortic tissue elastin. *J. Clin. Lab. Anal.* 9:293–296, 1995.
- <sup>30</sup>Oxlund, H., J. Manschot, and A. Viidik. The role of elastin in the mechanical properties of skin. *J. Biomech.* 21:213–218, 1988.
- <sup>31</sup>Perie, D., J. C. Iatridis, C. N. Demers, T. Goswami, G. Beaudoin, F. Mwale, and J. Antoniou. Assessment of compressive modulus, hydraulic permeability and matrix content of trypsin-treated nucleus pulposus using quantitative MRI. *J. Biomech.* 39:1392–1400, 2006.
- <sup>32</sup>Perie, D. S., J. J. Maclean, J. P. Owen, and J. C. Iatridis. Correlating material properties with tissue composition in enzymatically digested bovine annulus fibrosus and nucleus pulposus tissue. *Ann. Biomed. Eng.* 34:769–777, 2006.
- <sup>33</sup>Pezowicz, C. A., P. A. Robertson, and N. D. Broom. The structural basis of interlamellar cohesion in the intervertebral disc wall. *J. Anat.* 208:317–330, 2006.
- <sup>34</sup>Schmidt, H., A. Kettler, F. Heuer, U. Simon, L. Claes, and H. J. Wilke. Intradiscal pressure, shear strain, and fiber strain in the intervertebral disc under combined loading. *Spine* 32:748–755, 2007.
- <sup>35</sup>Schmidt, M. B., V. C. Mow, L. E. Chun, and D. R. Eyre. Effects of proteoglycan extraction on the tensile behavior of articular cartilage. *J. Orth. Res.* 8:353–363, 1990.
- <sup>36</sup>Smith, L. J., and N. L. Fazzalari. Regional variations in the density and arrangement of elastic fibres in the anulus fibrosus of the human lumbar disc. *J. Anat.* 209:359–367, 2006.
- <sup>37</sup>Stegemann, H. Microdetermination of hydroxyproline with chloramine-T and p-dimethylaminobenzaldehyde. *Hoppe Seylers Z. Physiol. Chem.* 311:41–45, 1958.
- <sup>38</sup>Szirmai, J. A. Structure of the intervertebral disc. In: *Chemistry and Molecular Biology of the Intercellular Matrix*, edited by E. A. Balazs. London: Academic Press, 1970, pp. 1279–1308.
- <sup>39</sup>Thompson, J. P., R. H. Pearce, M. T. Schechter, M. E. Adams, I. K. Tsang, and P. B. Bishop. Preliminary evaluation of a scheme for grading the gross morphology of the human intervertebral disc. *Spine* 15:411–415, 1990.
- <sup>40</sup>Tsantrizos, A., K. Ito, M. Aebi, and T. Steffen. Internal strains in healthy and degenerated lumbar intervertebral discs. *Spine* 30:2129–2137, 2005.
- <sup>41</sup>Tsuji, H., N. Hirano, H. Ohshima, H. Ishihara, N. Terahata, and T. Motoe. Structural variation of the anterior and posterior anulus fibrosus in the development of human lumbar intervertebral disc: a risk factor for intervertebral disc rupture. *Spine* 18:204–210, 1993.
- <sup>42</sup>Watanabe, T., K. Ishimori, A. J. Verplanke, H. Matsuki, and H. Kasuga. An enzyme-linked immunosorbent assay (ELISA) for the quantitation of urinary desmosine. *Tokai J. Exp. Clin. Med.* 14:347–356, 1989.
- <sup>43</sup>Yu, J., J. C. Fairbank, S. Roberts, and J. P. Urban. The elastic fiber network of the anulus fibrosus of the normal and scoliotic human intervertebral disc. *Spine* 30:1815–1820, 2005.
- <sup>44</sup>Yu, J., U. Tirlapur, J. Fairbank, P. Handford, S. Roberts, C. P. Winlove, Z. Cui, and J. P. Urban. Microfibrils, elastin fibres and collagen fibres in the human intervertebral disc and bovine tail disc. *J. Anat.* 210:460–471, 2007.
- <sup>45</sup>Yu, J., P. C. Winlove, S. Roberts, and J. P. Urban. Elastic fibre organization in the intervertebral discs of the bovine tail. *J. Anat.* 201:465–475, 2002.